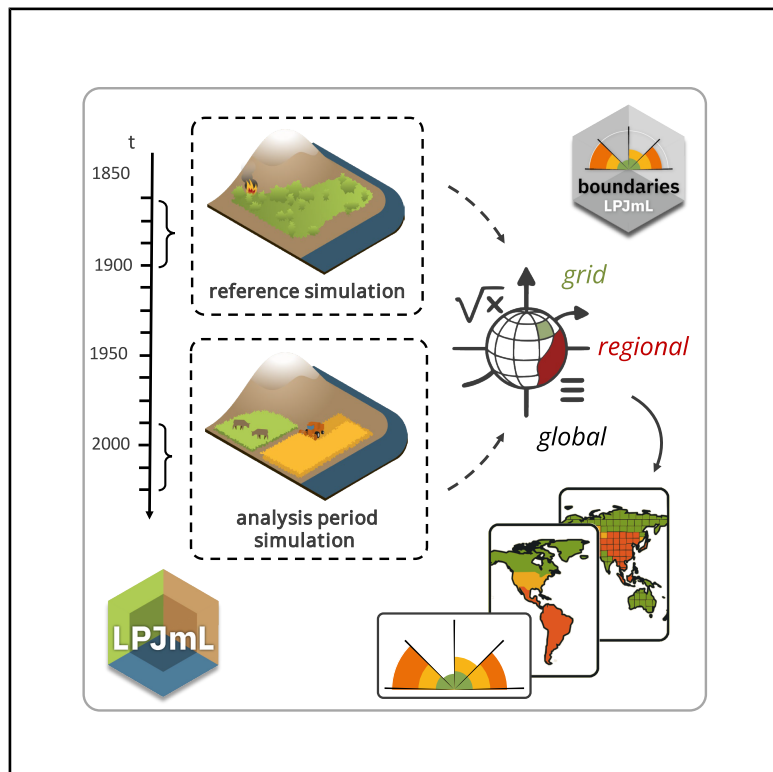


A software package for assessing terrestrial planetary boundaries

Graphical abstract



Highlights

- A software package has been developed to facilitate planetary boundary assessment
- An application translates LPJmL biosphere model outputs into boundary statuses
- The spatiotemporal transgression patterns of four boundaries is evaluated
- Guidance is provided for use of the tool with other models and datasets

Authors

Dieter Gerten, Johanna Braun,
Jannes Breier, Wolfgang Lucht,
Arne Tobian, Fabian Stenzel

Correspondence

dieter.gerten@pik-potsdam.de (D.G.),
johanna.braun@pik-potsdam.de (J.B.)

In brief

Planetary boundary (PB) assessments are hampered by the lack of a generic computation tool. Here we developed an R-based, open source software package, *boundaries*, that can calculate and visualize the spatiotemporal status of different PBs. Building on outputs from a biosphere model we demonstrate how the tool provides transparent and robust evaluation of PBs for land-system change, biosphere integrity, biogeochemical flows and freshwater change. Guidance is provided on how to use *boundaries* for processing outputs from other models and datasets.



Resource

A software package for assessing terrestrial planetary boundaries

Dieter Gerten,^{1,2,3,5,6,*} Johanna Braun,^{1,5,*} Jannes Breier,^{1,2,5} Wolfgang Lucht,^{1,2,3} Arne Tobian,^{1,4} and Fabian Stenzel^{1,4}

¹Research Department of Earth System Analysis, Potsdam Institute for Climate Impact Research (PIK), Member of the Leibniz Association, Potsdam, Germany

²Geography Department, Humboldt-Universität zu Berlin, Berlin, Germany

³RII THESys, Humboldt-Universität zu Berlin, Berlin, Germany

⁴Stockholm Resilience Centre, Stockholm University, Stockholm, Sweden

⁵These authors contributed equally

⁶Lead contact

*Correspondence: dieter.gerten@pik-potsdam.de (D.G.), johanna.braun@pik-potsdam.de (J.B.)

<https://doi.org/10.1016/j.oneear.2025.101341>

SUMMARY

There is a dearth of assessments of temporal trajectories and spatial patterns of planetary boundaries (PBs). However, a generic computation tool to facilitate such studies is lacking. Here, we developed an R-based, open-source software package “*boundaries*” that can calculate and plot the statuses of different PBs (i.e., if, when, where, and how strongly they are transgressed), based on required variables provided from an external source. The pilot version presented here is designed to use outputs from the LPJmL biosphere model, which dynamically simulates processes underlying the PBs for land system change, biosphere integrity, biogeochemical (nitrogen) flows, and freshwater change. We quantify and visualize the past and current statuses of these four PBs to demonstrate how *boundaries* can provide transparent and robust PB evaluation. We strongly encourage users to enhance *boundaries* for processing outputs from other models and datasets and provide guidance on how to do so.

INTRODUCTION

In the Anthropocene, humanity’s imprint on the Earth system is manifold and accelerating,¹ requiring solid knowledge of these impacts, their interactions, and eventually pathways toward a more sustainable future.² A specific challenge is to robustly quantify the processes that may lead to a rising risk of destabilization of planet Earth, integrating anthropogenic and natural changes in a common quantitative framework, and highlighting guardrails that should be maintained to avoid disastrous developments.

The planetary boundaries (PBs) framework^{3–5} is believed to be key to assessing and mitigating these planetary risks.⁶ The framework proposes quantitative limits to (human influence on) nine major Earth system processes, namely, climate change, stratospheric ozone depletion, ocean acidification, aerosol loading, biogeochemical flows, biosphere integrity, freshwater change, land system change, and novel entities. A chief assumption is that all PBs together delineate a safe operating space for humanity, characterized by a comparatively stable climate and biosphere as experienced during the Holocene epoch of the past approximately 11,700 years. It is the one and only Earth system state historically known to have supported civilization, agriculture, and, recently, a human population of billions of people. In accordance with applying a precautionary principle to matters of

existential risk, this safe space should be maintained, by respecting the PBs and their defining control variables, to avoid that Earth (or important subsystems) be put onto a trajectory that would undermine the ecological foundation of today’s complex human societies. The PBs are set at the lower end of a scientific uncertainty range (also called zone of increasing risk) regarding the magnitude and likelihood of such detrimental developments, to minimize the risk of their occurrence.³

While definitions and quantifications of the control variables are being continuously refined, recent assessments suggest that six of the nine PBs (all but those for ozone depletion, aerosol loading, and ocean acidification) are currently overstepped, some substantially.⁵ Some areas even face synchronous transgression of multiple PBs, due mainly to environmentally unsustainable agricultural practices.⁷ Many factors driving PB transgressions are still showing upward trends rather than stabilizing or declining ones.

The complex spatiotemporal patterns of relevant PB variables and their dynamic interaction network can only be captured with global observational datasets (partly unavailable or incomplete, and hardly explored yet) and models of the Earth system or subsystems of it. Such models have been used in a few cases to quantify PB statuses^{4,7,8} and selected PB interactions.^{5,9–11} However, their capacity to more comprehensively and regularly quantify Earth system states and feedbacks has not yet been



fully exploited in present-day PB analysis, which would also require the use of multiple models and datasets.¹² Moreover, there is no standardized analysis tool yet to rigorously assess PB statuses based on such data. Filling this research and development gap would be important to quantify and better understand drivers and magnitudes of historic, current, and potential future PB transgressions, including an exploration of humanity's options for returning to a safe and just space within all PBs.² In this context, it is also relevant to not only quantify the global but also the corresponding regional values defined for some PBs (e.g., continental forest biome area and grid cell-level environmental flow requirements representing regional land system and blue water change, respectively). One practical difficulty is that output from models principally suited for such analysis needs to be tailored for calculating PB statuses on par with updated definitions of the evolving framework. This requires representation of the control variables and the dynamics of their underlying processes in space and time, ideally accounting for process interactions; the flexibility to accommodate changes in definitions or scales of analysis as PB science is advancing; the provision and processing of required model output variables; and the representation of anthropogenic pressures upon PBs.

Here, we introduce an open source software package, *boundaries*, in support of such model implementations and analyses. This tool permits internally consistent, replicable and speedy calculation as well as visualization of dynamically changing statuses of different PBs. We use simulations from a terrestrial biosphere model (LPJmL) as input to demonstrate the package and also provide information for how to apply *boundaries* to models other than LPJmL. We account for the PBs for blue and green freshwater change, land system change, biosphere integrity, and nitrogen flows, all of which have been found to be transgressed in diverse studies,^{5,12–15} which we reassess and reconfirm here. The status of these PBs is quantified based on spatially distributed patterns of their control variables, the calculation of which requires a number of parameter specifications inflicted with uncertainties, necessitating transparent calculation and analysis schemes. In the following, we describe the *boundaries* package and its data inputs, and summarize how the PBs and their underlying processes are defined and computed in LPJmL. We also provide a technical and scientific validation demonstrating the functionality of the package and the plausibility of outputs delivered. In an example application, we evaluate the historic evolution of the calculated PBs' statuses, and map the contemporary regional distribution of their control variables. Overall, we present a PB analysis package that we believe helps to make PB science more transparent, and to reduce the risk of mistakes or misunderstandings by erroneous post-processing routines. We conclude with a discussion of the limitations of our present setup, options for improvement for general applicability, and opportunities for broader scientific applications of *boundaries* in global sustainability research.

RESULTS

Method summary

We developed the *boundaries* package for calculating and plotting the statuses and spatiotemporal transgression patterns of different PBs, by way of post-processing gridded global simula-

tions of PB-related variables from the Dynamic Global Vegetation Model LPJmL.^{16,17} The version presented and tested here accounts for the PBs for land system change, (functional) biosphere integrity, biogeochemical (nitrogen) flows, and freshwater change. LPJmL in combination with *boundaries* brings together conceptual, numerical, and technical advancements made since earlier publications.^{7,8,11,18} In essence, LPJmL simulates vegetation growth on natural and managed land coupled to biogeochemical, ecological, and hydrological processes. To facilitate flexible configuration of model runs (e.g., regarding simulated time periods, input data, and parameter settings), as well as data exchange to *boundaries*, we use the *lpjmlkit* software package described and provided elsewhere.¹⁹ Based on the required LPJmL model outputs, *boundaries* computes PB statuses and patterns over a given time period using its calculation, evaluation and plotting functions (Figure 1). A detailed description of *boundaries* and methods of its evaluation is given in the *methods* section.

Resource description

Technically, the current implementation of the *boundaries* software package is an R-based analysis tool that processes specific outputs from the LPJmL terrestrial biosphere model relevant for PB analysis. That model's general features have been described and evaluated before,^{16,20} while an updated version is used here (see *methods*). LPJmL simulates the growth and productivity of different vegetation types in coupling with ecological, biogeochemical, and hydrological processes, on a global grid and at daily time steps. Climate, land use, and certain parameters (such as for agricultural management) are prescribed as input to the model. A time period can be chosen to represent a Holocene-like reference state (the safe operating space for each PB considered) and, respectively, a subsequent analysis period of dynamically changing PB statuses in response to (mostly anthropogenic) drivers (Figure 1).

Required LPJmL output is then post-processed by *boundaries* so as to represent the PB control variables according to the chosen approach/definition, for the desired temporal and spatial scales—the package is currently designed to permit computation of PB statuses at grid cell, biomes/basins and global scale (Figure 1; Table 1). The *methods* section provides both a description of the package's functions and the calculation details for the individual PBs currently implemented, as used in our LPJmL simulation given the latest PB definitions (Table 1).

Technical validation

In the following, we present results from an application and output validity testing of *boundaries*. The software package itself contains a set of unit tests and integration tests for each PB calculation function, to ensure its overall technical and structural validity. In addition, as a scientific evaluation of the suitability of our method to assess PB statuses besides its mere technical capability, we provide a succinct comparison of key global PB (-related) variables computed by LPJmL with independent data sources, delivered by a *boundaries* evaluation function (Table 2).

This evaluation also serves as a basis for the application case study described in the following, aimed at comprehensively demonstrating *boundaries*' functionalities for computing spatial and temporal patterns of PB transgressions. In this application,

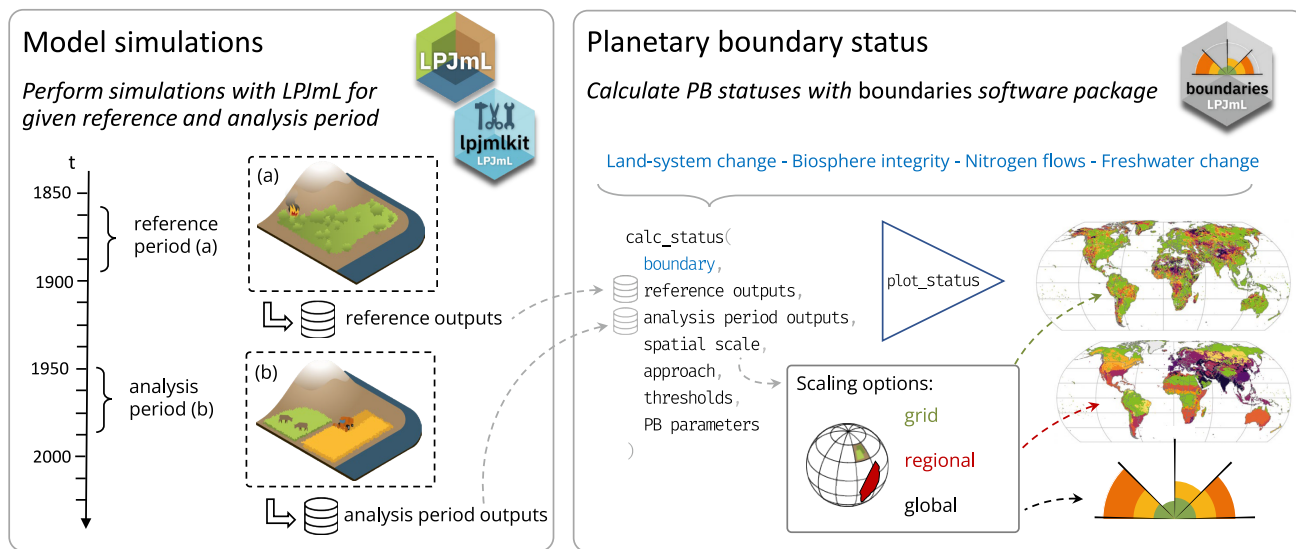


Figure 1. Overview of the basic workflow providing LPJmL biosphere model outputs (left) to the *boundaries* software package (right)

Outputs, i.e., PB control variables, are needed for a pre-industrial reference period and any later period for which PB statuses are to be analyzed. They are transformed by *boundaries* to PB statuses according to given PB definitions (approaches) and parameter thresholds, for different scales (grid, regional, global), and eventually plotted as maps or time series graphs.

we determined the annual values of the four PBs' control variables for the period 1901–2017 at the spatial scales specified in Table 1, relative to a pre-industrial reference state. To preserve internal consistency and comparability, the latter is represented under the same conditions for each PB, i.e., for the same reference period (200 years with recycled 1901–1930 climate), and assuming potential natural vegetation as computed by LPJmL absent anthropogenic land use, water use, or N deposition and application (details in methods).

Based on *boundaries*' functions, we then plotted the global PB statuses as historical trajectories (two alternative visualizations, spherical or cartesian, with or without moving average) (Figures 2A and 2B) and analyzed the regional patterns as maps for the most recent decade (Figure 3). The latter show the PBs for land system change and biosphere integrity at their typical operation scale, the biome level. Since a statistical method for defining green or blue water change has not yet been tested at the subglobal scale, we show grid-based blue water change using the earlier definition based on environmental flow requirements instead. Also, for nitrogen flows we show a grid resolution map, since there is no biome- or basin-scale status defined. For all available maps computed by the package, see Figure S1 (grid resolution) and S2 (regional resolution); Figure S3 shows the delineation of the spatial units (basins and biomes) underlying the respective calculations.

The spatial and temporal patterns found based on our simulation require in-depth analysis in further studies, yet here we give a brief overview on the results and a comparison with earlier findings. As Figure 2 shows, all four PBs analyzed are currently transgressed. But, the timing of the first transgressions differ substantially, as do the subsequent trajectories and the levels that the control variables eventually reach (within the increasing risk zone or the high-risk zone). Furthermore, blue and green freshwater change as well as biosphere integrity exhibit relatively

strong interannual fluctuations whereas nitrogen flows and land system change show a smooth development.

The land system change PB is found to be transgressed since the early 1930s, earlier than suggested before based on different input data and model parameterizations.⁵ The remaining potential forest cover is here computed to be 69% globally (Table 2), almost 10% higher than suggested by other studies, and also with differences at biome and regional level.^{11,12,35} Note however that our estimate tends to underestimate deforestation by approximately 10% because only agricultural areas are considered to reduce forest extent, while other drivers such as urban and infrastructure development are neglected.⁴² Also, forest loss after the period analyzed⁴² is not accounted for.

The biosphere integrity PB was overstepped over 100 years ago, with a human appropriation of net primary production (HANPP) of greater than 10% due to considerable land use already in those times (Figure 2). The value has been further increasing since, up to the current level of 18.4%, which is way beyond a precautionary PB aiming to safeguard the terrestrial biosphere's functional integrity due to widespread regional transgressions (Figure 3). This development largely agrees with earlier findings⁵ and has been further elaborated based on the same model and analysis tool^{15,21}; but, as we omit wood harvest, our estimate is lower and PB transgression commences later than found there (Table 2).

The transgression of the nitrogen PB has been continuously increasing since the mid-1960s, with only a short dip in the 1990s (Figure 2). This global trajectory largely agrees with earlier findings,^{5,43} albeit using different calculation approaches. As also confirmed by previous studies,^{5,14,43,44} the N boundary is now surpassed especially in parts of Europe, North America, and China (Figure 3), such that it is globally in the high-risk zone.

The PB for freshwater change is continuously overstepped—with the global land area affected by local streamflow or soil

Table 1. Definitions, values and spatial analysis scales of planetary and regional control variables considered

PB (reference)	0.5° grid cell scale	Regional scale	Global scale
Land-system change ⁴	remaining natural forest extent (w.r.t. the forest biome a cell belongs to): 85 (60)% boreal/tropical, 50 (30)% temperate%	remaining natural forest biome extent: 85 (60)% boreal/tropical, 50 (30)% temperate	remaining natural forest extent globally: 75 (60)%
Biosphere integrity ²¹	share of potential natural net primary production altered or prevented: 10 (20)%	same, aggregated to biome level	same, aggregated globally
Biogeochemical (N) flows ^{14,22}	mean annual N concentration in runoff to surface waters: 2 (5) mg N L ⁻¹	ND	global N surplus on agricultural areas: 35 (84) Tg yr ⁻¹
Freshwater change (blue water and green water) ^(23, alt; 13)	ND	ice-free land area with cell-scale transgressions beyond 5th/95th (50th) percentile of pre-industrial variability, at river basin scale	global ice-free land area with cell-scale transgressions beyond 5th/95th (50th) percentile of pre-industrial variability of this area
Freshwater change (earlier approach, blue water) ⁷	environmental flow requirements below: 75 (45)% of mean monthly flow for low-flow months; 60 (30)% for intermediate-flow months, 45 (15)% for high-flow months	ND	ND

Numbers in brackets: upper end of increasing risk zone leading to the high-risk zone. n.d. = not defined/used here.

moisture deviations being greater than in pre-industrial times—since before the onset of the 20th century, i.e., earlier than the years 1905 and 1929 noted before.²³ This can be explained by the fact that the other study used a larger model ensemble, different forcing datasets, and a different reference period with historic land use rather than potential natural vegetation. The magnitude of transgression is here found to be stronger, especially regarding the green water PB with currently approximately 31% of the global land area affected by soil moisture change (Table 2; Figure 3). As a cross-check, we processed the LPJmL data used in²³ with *boundaries* and found almost perfect agreement, which further proves the package's functionality as such. Moreover, testing the effect of alternative climate input datasets (monthly data from CRU⁴⁵) and reference periods shows that both the stepwise increase in blue and green water departures around 1925 and the transgression magnitudes are much less pronounced (see Figure S4). However, also the nitrogen boundary status is different (less severe and in the high-risk zone only since 2010) in this simulation, probably related to higher plant productivity and thus higher nitrogen removals from harvesting. These differences point to the need to use multiple inputs in future assessments.

For reasons of comparison we include the climate change PB in the overview in Figure 2B, using atmospheric CO₂ concentration as one of its two control variables. Owing to continued greenhouse gas emissions during the past decades, this PB has been transgressed for the first time in 1986 (>350 ppm) and has steadily moved further into the increasing risk zone since, reaching 419 ppm in 2023.⁴⁶

Limitations

While the *boundaries* software package presented here is operational as shown above, it is built around outputs from the LPJmL

terrestrial biosphere model, not covering PBs related to oceans and the atmosphere. However, the package design can in principle be expanded for inclusion of other PBs to eventually represent all nine of them collectively, as long as their control variables are delivered by global datasets from observations or modelings (see below). Such an expansion can be facilitated e.g., by providing all data in a common format such as netCDF. Moreover, the package design and functionality allows further enhancements such as regarding spatial aggregation levels, visualizations and color schemes including color-blind options^{47,48} or any details of PB calculation.

DISCUSSION

Comparison with existing approaches and resources

We here present the *boundaries* software package for calculating the status and spatiotemporal evolution of multiple PBs and provide it as an open source tool to the scientific community for further use and enhancement, in support of PB science. In future applications, in conjunction with either the LPJmL model (as herein) or other models and datasets, we envisage it to become a key tool for advancing the quantification of global and regional PB processes, statuses, and interactive effects. The PBs are defined to demarcate a safe operating space for the entire humanity. Therefore, an improved understanding based on latest data, models, and analysis tools is crucial for understanding potential future trajectories of the Anthropocene and developing appropriately founded governance for critical planetary commons in response.⁴⁹

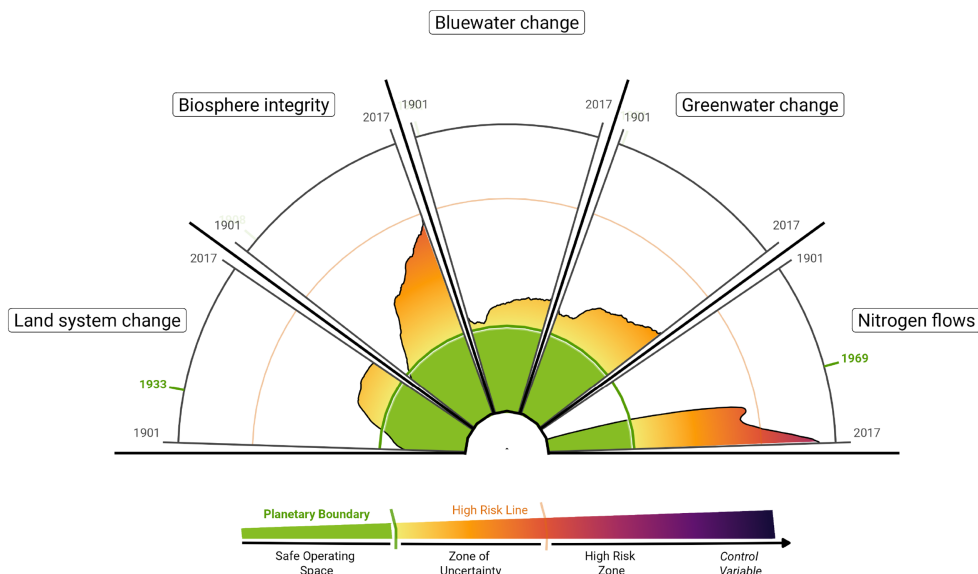
The pilot application and evaluation presented here demonstrates that *boundaries* is suited for internally consistent and transparent assessment of PB statuses, their spatial patterns, and their trajectories over time, advancing earlier approaches

Table 2. Global values of PB-relevant variables from the LPJmL model simulation as derived from *boundaries's validation function*, compared to estimates from independent studies (grouped by PBs for which they are most relevant)

Variable	Unit	Value, this paper	Range, other estimates [year]
Land-system change PB			
Cropland area*	Mha	1,556	1,550 [2015] ²⁴ 1,572–1,604 [2015] ²⁵
Pasture area*	Mha	3,267	3,181 [2015] ²⁴ 3,241 [2015] ²⁵
Potential natural forest extent	Mha	5,492	5,737 ²⁶
Deforested area	% of pot. extent	31	25 [2019] ²⁶ 40 [2020] ⁵
PB status	% remaining forest	69	59 [2020] ⁵ 60 [2023] ¹²
Functional biosphere integrity PB			
Crop production for all explicitly modeled crop types	Gt fresh matter	4.595	6.397 [2015] ²⁷ for all crops
PB status	% HANPP of pre-industrial NPP	18.4	20–25 [2007–2016] ²¹ 30 [2020] ⁵ 20.7 [2010] (²⁸ ; under current climate)
Freshwater change PB			
Irrigated area*	Mha	263	255 [2005] ²⁹ 314 [2005] ³⁰ 367 [1999–2012] ³¹ – incl. areas equipped for irrigation
Irrigation water withdrawals	km ³ yr ⁻¹	2,273	1,867 [2005] ³² 2,158–3,185 [various recent periods] (³³ using different sources) 2,148–3,232 [various recent periods] (³⁴ using different sources)
Irrigation water consumption	km ³ yr ⁻¹	840	874 [2005] ³² 1,035–1,368 [various recent periods and sources] ³⁴
PB status—blue water (area with discharge deviation)	% of ice-free area	20.6	18.2 [1996–2005] ²³
PB status—green water (area with soil moisture deviation)	% of ice-free area	30.6	15.8 [1996–2005] ²³
Biogeochemical flows (nitrogen) PB			
N use efficiency on cropland	%	52	46 (40–53) [2010] ³⁵
N surplus on cropland	Tg N yr ⁻¹	79	86 (68–97) [2010] ³⁵ 93 [2000] ³⁶
N fertilizer application	Tg N yr ⁻¹	99	98 [2011–2015] ³⁵
N manure application	Tg N yr ⁻¹	17.2	27 [2018] ³⁷ 22 [2011–2015] ³⁵
N leaching (total)	Tg N yr ⁻¹	77	93 [2000] ³⁶ 86 [1990] ³⁸
N leaching from cropland	Tg N yr ⁻¹	44	48.5 [2010] (after) ³⁹ 42.9 [2010] (after) ⁴⁰
PB status	Tg N yr ⁻¹	95	119 [2010] ¹⁴

Note that model results are averaged over the time period 2005–2014, whereas other estimates are mostly for particular years within and around this period. Key land use-related inputs to LPJmL are also included as their uncertainties potentially affect the estimation of PB statuses (marked by an asterisk; from⁴¹ and references therein).

A



B

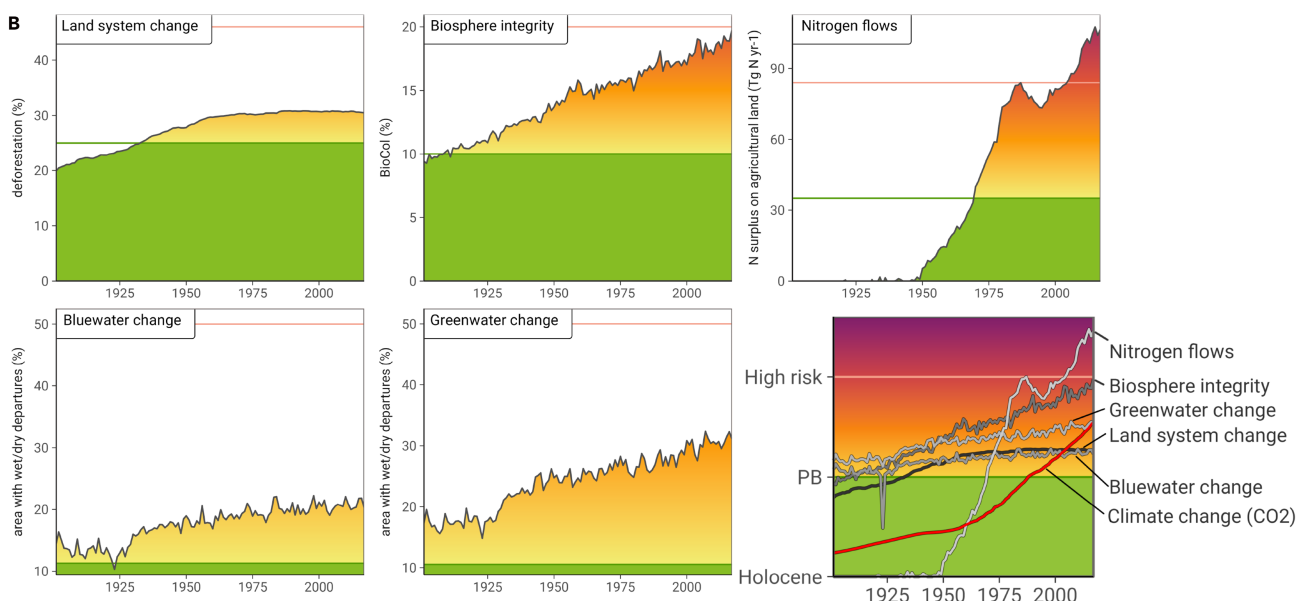


Figure 2. Temporal evolution (1901–2017) of annual statuses of the PBs considered, computed by boundaries based on LPJmL model outputs

There are two alternative visualization options.

(A) Wedges diagram depicting the trajectories of the control variables for each PB (10-year moving averages, normalized units).

(B) Time series of the PB control variables individually (original units) and combined into one plot (bottom right; normalized values as in (A), additionally including atmospheric CO₂ concentrations, a control variable of the climate change PB). All plots depict when a control variable was still in the safe space (green) and when the PB was transgressed reaching the zones of increasing or high risk, respectively. Values have been normalized for the safe zone based on the respective Holocene and PB values, and, if the PB is transgressed, based on the increasing risk zone.

in which individual or multiple PBs were analyzed in separate studies or with separate scripts that are not stored at a central place and make it difficult to trace and reproduce calculation details. We consider this to be a major improvement on earlier attempts to quantify and visualize PB trajectories, as provided in

the appendix to⁵⁰ or on websites such as <https://globalaia.org/boundaries> and <https://planetaryboundaries.kcvs.ca>. These sources seem to have used dispersed datasets lacking internal consistency across PBs, and the original data sources as well as the calculation details are not fully documented. Using our

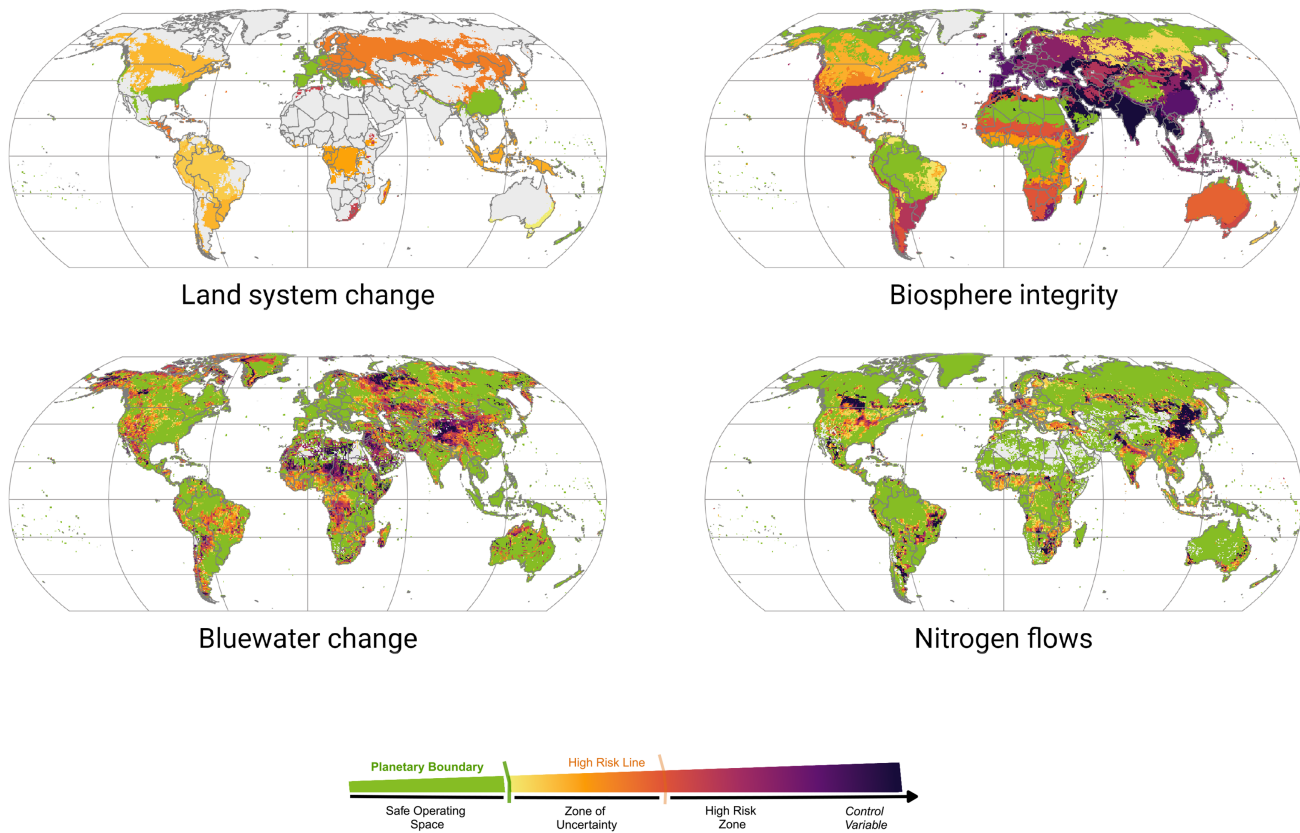


Figure 3. Regional transgression patterns of the four PBs considered for the 2008–2017 decade, computed and mapped with *boundaries* based on LPJmL model outputs

The maps display safe, increasing risk, and high-risk areas, exemplarily at biome scale (land system change, biosphere integrity) and 0.5° grid cell scale (freshwater/blue water change, biogeochemical/nitrogen flows), respectively. Light gray colored cells indicate where PB definitions do not apply (i.e., land system change, non-forest biomes; biosphere integrity and freshwater change, permanent ice areas).

software provides a transparent way of calculating different PBs, as any details of calculation can be configured and documented. Also, an interface to data sources, here the LPJmL model, is provided, facilitating the incorporation of required data fields into *boundaries* for subsequent analysis. As this tool is unique so far, a more elaborated comparison with previous resources is not feasible. In the following, we discuss further possibilities to enhance the software and use it for scientific studies.

Prospects for enhancement and broader future applications

To keep up with scientific progress, advancements in PB value setting (i.e., where to set the PB) can be easily considered in the *boundaries* software by changing function parameters. Also, the structure of the package is designed to allow for straightforward integration of alternative and upcoming new PB definitions based on new sub-functions (including, e.g., a representation of the somewhat different Earth system boundaries²² or food system-related PBs used by the EAT-Lancet commission⁵¹). This includes readiness for scaling from grid cell level to biome or river basin level to global level, with an openness to including other spatial aggregation units as well.⁵² Flexible methods for such scaling of PBs are eventually also suited for PB operationalization, i.e., the translation of countries'

or business companies' shares to PB transgression and maintenance.⁵³

While the software is tested here based on a particular LPJmL model simulation, its design allows for the processing of different model runs and their joint analysis and visualization. For instance, by keeping certain drivers or, respectively, the status of certain PBs constant in a simulation, *boundaries* can be used to isolate the drivers' individual influences on PB statuses.⁵⁴ Such analyses would be important, as studies suggest that PB transgressions may negatively affect the status of respective other PBs.^{55,56}

That said, *boundaries* allows for more elaborate mapping and interpretation of spatiotemporal patterns (including use of input from further sources and systematic uncertainty analyses) than we can demonstrate in this paper. Regarding the use of LPJmL as such, this model is now being coupled into the wider Potsdam Earth Model, allowing to represent mutual feedbacks between the bio- and atmosphere.⁵⁷ This model system will enable endogenous representation of the climate change PB and its interactions with other PBs, such as initially demonstrated for the land system change PB⁵ and potentially for other land-related PBs.⁵⁸ Besides, *boundaries* can call other software prepared to calculate individual features, such as done here by linking the *biospheremetrics* package²¹ and prospectively by linking

Box 1. Enhancing boundaries for multi-model compatibility

To use simulation data from models other than LPJmL (e.g., other dynamic global vegetation models, global hydrological models, Earth system models) as input to *boundaries*, the variables for computing the respective control variables need to be represented, along with their spatial and temporal dynamics. Table S1 gives an overview of required variables for each PB, and their congruency with variables from ISIMIP⁶⁰ chosen as an example case here, as it provides a framework for harmonizing climate impact simulations across models and sectors. While *boundaries* relies on the *lpjmlkit* R package for reading in and processing model-specific outputs, we provide an enhanced *lpjmlkit* version (v1.7.7-boundaries.0) to support files in the widely used and standardized netCDF format following ISIMIP conventions.¹⁹ It is thus in principle suitable for outputs from any Earth (sub-)system model. Aspired full compatibility of *boundaries* with model data following ISIMIP standards would allow for more reliable model ensemble analysis. However, this requires additional functionality for a generic transfer of meta-information (simulation period, simulation outputs, etc.) to *boundaries* not provided in the present version. Also, structural adjustments in some PB status functions are needed to make calculations compatible e.g., with varying output structures, particularly for outputs that differentiate plant functional types that vary in number and definition across models. Our present *boundaries* version already provides functionality to map plant types to common categories for multi-model compatibility of the subsequent calculations. In general, the structure of the package is designed to allow for straightforward integration of new calculation functions not limited to only terrestrial PBs. It also provides an interface to make any global time series of PB variables compatible with the *boundaries* plotting functions (independent of using the *calc_status* function). The *boundaries* github repository will serve as a platform for future continuous development including enhancing model applicability and PB coverage as part of a community effort.

to an additional tool for systematically assessing interactive effects of different PB statuses.¹¹ Inter-comparative use of different input datasets and models is advised, as previous studies indicate rather pronounced differences in PB statuses depending on which resources and basic datasets have been used for their calculation and mapping (compare, e.g., maps in Steffen et al.^{4,7} and Gerten et al.,^{4,7} and our comparisons above). To facilitate usage of the software for processing other models' outputs, Box 1 provides guidance and materials. Rigid confidence assessment and evaluation against observations is required for different PB-related variables—going beyond a validation of global quantities as in Table 2—if a next generation of multi-source, uncertainty-controlled PB assessments is to be developed. This will ideally happen in a manner that connects to internationally coordinated scenario analysis for the Intergovernmental Panel on Climate Change including multi-model assessments such as by the ISIMIP The Inter-Sectoral Impact Model Intercomparison Project (<https://www.isimip.org>). Furthermore, the software can potentially be used in more encompassing scenarios analyses of how to maintain PBs, return into the safe space, and achieve social goals within PBs.^{7,59} They may therefore contribute to providing a scientific foundation also for framing a next generation of Sustainable Development Goals for after 2030.

METHODS

Method details

LPJmL model, simulations, and inputs

We here use version 5.8.11 of the LPJmL biosphere model, which includes updates of multiple components of the latest main version 5.0,^{16,20} i.e., a representation of the nitrogen cycle¹⁷ and further improvements of crop management, biological nitrogen fixation, and livestock grazing.^{21,61} LPJmL simulates the growth and productivity of 11 natural and 12 crop functional vegetation types, as well as managed grasslands, each agricultural type assumed to be either irrigated or rainfed. Simulations are typically performed on a global 0.5° grid at daily resolution.

Model runs are forced by datasets on drivers not endogenously represented, such as climate, land use, non-irrigation water use, N deposition, and fertilizer application. Following a spin-up period that equilibrates natural vegetation and carbon pools, transient simulations are performed over a given time period capturing past and potential future climate and land use change effects.

For the specific application described in the main text, a transient model simulation was performed encompassing a reference period up to the analysis period 1901–2017. The reference state is chosen to be a 200-year time frame with pre-industrial (1841) atmospheric CO₂ concentration and randomly shuffled 1901–1930 climate (since climate data before that time are less reliable), assuming potential natural vegetation as simulated by the model. Specifically, we used global gridded climate data from GWSP3-W5E5^{62,63} and annual atmospheric CO₂ concentrations from,⁴⁶ which also extend to the analysis period 1901–2017. The simulation was preceded by a 3,500-year model spin-up under potential natural vegetation and subsequently under transient land use from 1500 to 2017. The gridded land use input data differentiate irrigated and rainfed areas, and they consider crop-specific fertilizer and manure applications.⁴¹ While irrigation water use is modeled by LPJmL, water use for other sectors (1900–2000, held constant thereafter) is taken from Flörke et al.⁶⁴ Agricultural management settings prescribed are tillage (1974–2010, constant thereafter⁶⁵); residue removal rates (1850–2015, held constant for the following years⁴⁰); and livestock densities, calibrated to match grazing intensities for 2000.^{21,66,67} Sowing dates and phenological heat units are internally computed; no intercropping is assumed.

PB definitions and calculations

The PB for land system change⁴ formulates limits to deforestation that safeguard the role of forest biomes particularly in climate regulation. The control variable is the fractional area of natural forest to be preserved, with the PB set to a value of 75% globally (Table 1). Biome-specific boundaries are higher for tropical and boreal forest than for temperate forest, due to their large-scale importance for moisture recycling and albedo,

respectively. The status of this PB is given by the remaining forest cover vs. its potential natural extent. Here, these areas are determined by subtraction of the annual area covered by pasture and cropland from the area modeled to be covered by potential natural vegetation in the reference period (as in¹¹). For the spatial aggregation to biome level, a grid cell is counted as forested if more than 60% of its area is covered by woody vegetation, following the International Geosphere-Biosphere Program land cover classification system (however, in view of the multitude of forest definitions, this threshold can be changed flexibly). The cell is then classified as either tropical, temperate, or boreal forest based on the simulated dominant tree type.

The PB for biosphere integrity is calculated following a proposal for a new control variable BioCol by Stenzel et al.,²¹ as suggested by Richardson et al.,⁵ modeled based on the HANPP.⁶⁸ HANPP is taken as a proxy for human interference with the energy flows available to the biosphere for producing its planetary functions. It is calculated as the sum of net primary productivity directly removed by harvesting of biomass and the amount altered or prevented due to human interference with the vegetation compared to pre-industrial potential natural vegetation. Other than in Stenzel et al.,²¹ where it was an external input, wood harvest is neglected here. Provisionally, the PB is set at 10% of Holocene net primary production (NPP),⁵ on the basis of current values of BioCol being associated with a multitude of indicators of biosphere integrity that today have strongly negative values and trends. BioCol can be computed at any scale; here, biome- and global-level values are considered by aggregating grid cell values and applying the same PB thresholds.

The PB for freshwater change accounts for changes in both blue water (streamflow) and green water (root zone soil moisture). While the former sustains aquatic and coastal biodiversity as well as biogeochemical cycling in riverine ecosystems, the latter maintains terrestrial ecosystems, sustains the land carbon sink and supports atmospheric moisture recycling. Freshwater change is considered to be beyond Holocene variability if, respectively, blue or green water in a month is below the 5th (dry departure) or above the 95th percentile (wet departure) of the respective month in the reference period.²³ If the annual mean area with monthly wet and/or dry departures, at river basin or global scale, exceeds the 95th percentile of the respective mean area in the reference period, the PB is considered to be transgressed. To account for a former approach used in a number of studies (e.g., Steffen et al.,^{4,7,18,69} Gerten et al.,^{7,18} and Virkki et al.^{4,7,18,69}) boundaries also computes rivers' environmental flow requirements and their transgressions after a variant of the Variable Monthly Flow method.^{7,70} This indicates a local boundary transgression if cell-based monthly streamflow is below pre-industrial mean monthly discharge computed for low-, intermediate-, and high-flow months (Table 1). To calculate the yearly PB status, the degree of exceedance is displayed as a fraction of the increasing risk range averaged over all months with a transgression (safe, <0.25; high risk, >0.75⁴).

Finally, regarding the PB for biogeochemical flows, *boundaries* currently considers nitrogen (N) flows only, as phosphorus is not yet represented in LPJmL. We focus on limits to surface water eutrophication as a major concern regarding anthropogenic modifications of the N cycle.⁴ Following updated con-

cepts,^{14,71} we define N boundaries for each grid cell based on critical N concentrations carried by (sub)surface runoff to surface streams. The boundary is considered transgressed when N concentration exceeds 1 mg N L^{-1} .⁷² Assuming that on average half of N flowing into surface waters is retained or sedimented, the control variable is given as the N concentration in runoff with its critical value set to 2 mg N L^{-1} . Point sources of N such as from sewage and aquaculture are presently not accounted for. These gridded concentration values cannot be simply aggregated to a global status.¹⁴ We therefore define the global N boundary based on N surplus on agricultural areas (N inputs from fertilizer, manure, deposition, seeds, and biological nitrogen fixation minus harvested N), assuming values in Rockström et al.,²² based on critical N deposition in terrestrial ecosystems in addition to surface water eutrophication thresholds (Table 1).

Functions of the resource

boundaries reads in (based on user-friendly functions from *lpjmlkit*), and then processes, the LPJmL simulation outputs for the reference and analysis period. The core wrapper function 'calc_status' calls internal PB-specific functions for computing the respective control variable states (yet for biosphere integrity the external 'biospheremetrics' R package is called, a stand-alone LPJmL-based tool²¹). For flexible application, the following options and basic parameters can be defined in 'calc_status' (Figure 1).

- (1) PBs for which to compute the status, i.e., the trajectory and spatial pattern of the control variable(s);
- (2) Reference and analysis time periods to apply;
- (3) Calculation approach complying with chosen PB definitions, including setting values for parameters on details of calculation;
- (4) Thresholds for converting the control variable state to a PB status;
- (5) Spatial scale of the calculation (global, regional, and grid cell levels).

Based on the outputs of this function, two further functions provide.

- (6) Plots and their layout (e.g., maps, time series, and possibly normalization of values);
- (7) a comparison of simulated global PB(-related) variables to independent data sources.

With regard to the time frames (2), *calc_status* allows computation of both the averaged PB status over a desired (multi-year-/decadal) analysis period and a time series of its long-term trajectory (annual values, possibly with a defined moving average). A specific approach to calculate a PB status can be selected (3) in that different calculation schemes or control variables are considered as proposed in current literature. In so doing, some model-specific parameters not prescribed or detailed in those definitions can be chosen, such as the minimum tree cover to define forests for the land-system change PB, or whether very dry areas should be excluded for calculation of the freshwater and nitrogen PBs. One can also (4) flexibly determine at which value a control variable equals the PB or the transition from the PB's zone of increasing risk to the high-risk zone, as some of

these thresholds are also still under debate. Eventually, the function `calc_status` returns the values of the control variables for the given PBs at the defined spatial resolution (5).

The `plot_status` function (6) illustrates the PB states as maps based on the chosen spatial aggregation level, as individual or combined time series, or as a chronological version of the standard wedges diagram used in previous publications that incorporates the temporal development—a layout we newly introduce here (Figure 2). All graphics depict whether a certain time period is in the safe zone, the zone of increasing risk or the high-risk zone, respectively, based on the defined thresholds and using a gradual, perceptually uniform color scheme similar to the ones used in latest publications.⁵ For this conversion of control variable values to the PB states, values are normalized for the safe zone based on the respective Holocene and PB values, and, if the PB is transgressed, based on the increasing risk zone, delimited by the PB and the high risk value (i.e., the transition from the increasing risk to the high risk zone). The trajectories of PBs can be plotted individually or in a plot combining multiple PBs, showing discrete years or moving averages. Maps also show the risk level of regions, and the desired projection of maps can be chosen. Variables determining the control variables can also be plotted, in case needed for in-depth analysis.

The `validate_simulation` function allows for (7) testing the sensitivity of results to different definitions and data used by comparing simulated global PB(-related) variables to independent data sources in tabular format. Additionally, unit and integration tests can be performed to ensure technical and structural validity based on the `test` function of the `devtools` R package.⁷³ For further documentation of details, see the publication of the code itself.⁷⁴

RESOURCE AVAILABILITY

Lead contact

Requests for further information should be directed to the lead contact, Dieter Gerten (dieter.gerten@pik-potsdam.de).

Materials availability

No new materials were generated in this study.

Data and code availability

The original code of the `boundaries` package (version 1.3.1) is deposited and publicly available at <https://doi.org/10.5281/zenodo.14906079> and on GitHub (<https://github.com/pik-tess/boundaries>), including a vignette with application examples. The enhanced `lpjmlkit` version (v1.7.7-boundaries.0) is published in a similar way at <https://doi.org/10.5281/zenodo.14850990>. The data and scripts used to demonstrate its functionality are publicly available at <https://doi.org/10.5281/zenodo.14906293>.

ACKNOWLEDGMENTS

Both D.G. and J. Braun are corresponding authors because of their different roles (main responsibility for manuscript writing and software development, respectively). We thank Caterina Vanelli for helping to develop the validation and plotting functions. The work received financial support from the European Union's Horizon 2020 Research and Innovation Programme (NEGEM project, grant agreement no. 869192) and the Horizon 2.5 Climate, Energy and Mobility Programme (WorldTrans project, grant agreement no. 101081661); the Generation Foundation, and Partners for a New Economy via the 'Earth4all' project; the European Research Council via the 'Earth Resilience in the Anthropocene' project (No. ERC-2016-ADG-743080); the Global Challenges Foundation via

the Future Earth project fund 'New Governance Architecture for Addressing Global Systemic Risks'; and the FORMAS project ReForMit. J. Braun's contribution is part of the Planetary Boundaries Science Lab's research effort at PIK, which is funded by The Grantham Foundation for the Protection of the Environment. The authors gratefully acknowledge the Ministry of Research, Science and Culture (MWFK) of Land Brandenburg for supporting this project by providing resources on the high-performance computer system at the Potsdam Institute for Climate Impact Research. We thank two anonymous reviewers and the editor for their valuable comments.

AUTHOR CONTRIBUTIONS

D.G.: conceptualization, methodology, writing (draft preparation, review, editing), funding acquisition; J. Braun: conceptualization, methodology, formal analysis, software, validation, visualisation, writing (review, editing); J. Breier: conceptualization, methodology, software, visualisation, writing (review, editing); W.L.: writing (review, editing); A.T.: methodology, writing (review, editing); F.S.: conceptualization, methodology, supervision, software, writing (review, editing).

DECLARATION OF INTERESTS

The authors declare no competing interests.

SUPPLEMENTAL INFORMATION

Supplemental information can be found online at <https://doi.org/10.1016/j.oneear.2025.101341>.

Received: June 21, 2024

Revised: November 26, 2024

Accepted: May 19, 2025

Published: June 13, 2025

REFERENCES

1. Steffen, W., Broadgate, W., Deutsch, L., Gaffney, O., and Ludwig, C. (2015). The trajectory of the anthropocene: the great acceleration. *Anthropocene Rev.* 2, 81–98. <https://doi.org/10.1177/2053019614564785>.
2. Rockström, J., Gupta, J., Lenton, T.M., Qin, D., Lade, S.J., Abrams, J.F., Jacobson, L., Rocha, J.C., Zimm, C., Bai, X., et al. (2021). Identifying a safe and just corridor for people and the planet. *Earths Future* 9, e2020EF001866. <https://doi.org/10.1029/2020EF001866>.
3. Rockström, J., Steffen, W., Noone, K., Persson, Å., Chapin, F.S., Lambin, E.F., Lenton, T.M., Scheffer, M., Folke, C., Schellnhuber, H.J., et al. (2009). A safe operating space for humanity. *Nature* 461, 472–475. <https://doi.org/10.1038/461472a>.
4. Steffen, W., Richardson, K., Rockström, J., Cornell, S.E., Fetzer, I., Bennett, E.M., Biggs, R., Carpenter, S.R., Vries, W.d., Wit, C.A.d., et al. (2015). Planetary boundaries: Guiding human development on a changing planet. *Science* 347, 1259855. <https://doi.org/10.1126/science.1259855>.
5. Richardson, K., Steffen, W., Lucht, W., Bendtsen, J., Cornell, S.E., Donges, J.F., Drücke, M., Fetzer, I., Bala, G., von Bloh, W., et al. (2023). Earth beyond six of nine planetary boundaries. *Sci. Adv.* 9, eadh2458. <https://doi.org/10.1126/sciadv.adh2458>.
6. Rockström, J., Donges, J.F., Fetzer, I., Martin, M.A., Wang-Erlandsson, L., and Richardson, K. (2024). Planetary Boundaries guide humanity's future on Earth. *Nat. Rev. Earth Environ.* 5, 773–788. <https://doi.org/10.1038/s43017-024-00597-z>.
7. Gerten, D., Heck, V., Jägermeyr, J., Bodirsky, B.L., Fetzer, I., Jalava, M., Kummu, M., Lucht, W., Rockström, J., Schaphoff, S., et al. (2020). Feeding ten billion people is possible within four terrestrial planetary boundaries. *Nat. Sustain.* 3, 1–9. <https://doi.org/10.1038/s41893-019-0465-1>.

8. Heck, V., Gerten, D., Lucht, W., and Popp, A. (2018). Biomass-based negative emissions difficult to reconcile with planetary boundaries. *Nat. Clim. Chang.* 8, 151–155. <https://doi.org/10.1038/s41558-017-0064-y>.
9. Andries, J.M., Barfuss, W., Donges, J.F., Fetzer, I., Heitzig, J., and Rockström, J. (2023). A modeling framework for World-Earth system resilience: exploring social inequality and Earth system tipping points. *Environ. Res. Lett.* 18, 095001. <https://doi.org/10.1088/1748-9326/ace91d>.
10. Lade, S.J., Fetzer, I., Cornell, S.E., and Crona, B. (2021). A prototype Earth system impact metric that accounts for cross-scale interactions. *Environ. Res. Lett.* 16, 115005. <https://doi.org/10.1088/1748-9326/ac2db1>.
11. Tobian, A., Gerten, D., Fetzer, I., Schaphoff, S., Andersen, L.S., Cornell, S., and Rockström, J. (2024). Climate change critically affects the status of the land-system change planetary boundary. *Environ. Res. Lett.* 19, 054060. <https://doi.org/10.1088/1748-9326/ad40c2>.
12. Caesar, L., Sakschewski, B., Andersen, L.S., Beringer, T., Braun, J., Dennis, D., Gerten, D., Heilemann, A., Kaiser, J., Kitzmann, N.H., et al. (2024). Planetary Health Check, 2024 (Potsdam Institute for Climate Impact Research. Technical report).
13. Wang-Erlandsson, L., Tobian, A., van der Ent, R.J., Fetzer, I., te Wierik, S., Porkka, M., Staal, A., Jaramillo, F., Dahlmann, H., Singh, C., et al. (2022). A planetary boundary for green water. *Nat. Rev. Earth Environ.* 3, 380–392. <https://doi.org/10.1038/s43017-022-00287-8>.
14. Schulte-Uebbing, L.F., Beusen, A.H.W., Bouwman, A.F., and de Vries, W. (2022). From planetary to regional boundaries for agricultural nitrogen pollution. *Nature* 610, 507–512. <https://doi.org/10.1038/s41586-022-05158-2>.
15. Stenzel, F., Ben Uri, L., Braun, J., Breier, J., Erb, K.H., Gerten, D., Haberl, H., Matej, S., Milo, R., Ostberg, S., et al. (2024). Mapping the Transgression of the Planetary Boundary for Functional Biosphere Integrity. *SSRN*. <https://doi.org/10.2139/ssrn.4998602>.
16. Schaphoff, S., von Bloh, W., Rammig, A., Thonicke, K., Biemans, H., Forkel, M., Gerten, D., Heinke, J., Jägermeyr, J., Knauer, J., et al. (2018). Lpjml4 – a dynamic global vegetation model with managed land – part 1: Model description. *Geosci. Model Dev. (GMD)* 11, 1343–1375. <https://doi.org/10.5194/gmd-11-1343-2018>.
17. von Bloh, W., Schaphoff, S., Müller, C., Rolinski, S., Waha, K., and Zaehle, S. (2018). Implementing the nitrogen cycle into the dynamic global vegetation, hydrology, and crop growth model LPJmL (version 5.0). *Geosci. Model Dev. (GMD)* 11, 2789–2812. <https://doi.org/10.5194/gmd-11-2789-2018>.
18. Gerten, D., Hoff, H., Rockström, J., Jägermeyr, J., Kummu, M., and Pastor, A.V. (2013). Towards a revised planetary boundary for consumptive freshwater use: role of environmental flow requirements. *Curr. Opin. Environ. Sustain.* 5, 551–558. <https://doi.org/10.1016/j.cosust.2013.11.001>.
19. Breier, J., Ostberg, S., Wirth, S.B., Höttgen, D., Minoli, S., Stenzel, F., and Müller, C. (2024). Ipjmikit: A toolkit for operating LPJmL and model-specific data processing. *J. Open Source Softw.* 9, 5447. <https://doi.org/10.21105/joss.05447>.
20. Schaphoff, S., Forkel, M., Müller, C., Knauer, J., von Bloh, W., Gerten, D., Jägermeyr, J., Lucht, W., Rammig, A., Thonicke, K., et al. (2018). LPJmL4 – a dynamic global vegetation model with managed land: Part II – model evaluation. *Geosci. Model Dev. Discuss. (GMDD)* 2018, 1–41. <https://doi.org/10.5194/gmd-2017-146>.
21. Stenzel, F., Braun, J., Breier, J., Erb, K., Gerten, D., Heinke, J., Matej, S., Ostberg, S., Schaphoff, S., and Lucht, W. (2024). biospheremetrics v1.0.2: an r package to calculate two complementary terrestrial biosphere integrity indicators – human colonization of the biosphere (biocol) and risk of ecosystem destabilization (ecorisk). *Geosci. Model Dev. (GMD)* 17, 3235–3258. <https://doi.org/10.5194/gmd-17-3235-2024>.
22. Rockström, J., Gupta, J., Qin, D., Lade, S.J., Abrams, J.F., Andersen, L.S., Armstrong McKay, D.I., Bai, X., Bala, G., Bunn, S.E., et al. (2023). Safe and just Earth system boundaries. *Nature* 619, 102–111. <https://doi.org/10.1038/s41586-023-06083-8>.
23. Porkka, M., Virkki, V., Wang-Erlandsson, L., Gerten, D., Gleeson, T., Mohan, C., Fetzer, I., Jaramillo, F., Staal, A., te Wierik, S., et al. (2024). Notable shifts beyond pre-industrial streamflow and soil moisture conditi-
- tions transgress the planetary boundary for freshwater change. *Nat. Water* 2, 262–273. <https://doi.org/10.1038/s44221-024-00208-7>.
24. FAO (2023). Faostat. <https://www.fao.org/faostat/en/#data/RL> [Accessed: (2024-06-13)].
25. Klein Goldewijk, K., Beusen, A., Doelman, J., and Stehfest, E. (2017). Anthropogenic land use estimates for the holocene – hyde 3.2. *Earth Syst. Sci. Data* 9, 927–953. <https://doi.org/10.5194/essd-9-927-2017>.
26. Grantham, H.S., Duncan, A., Evans, T.D., Jones, K.R., Beyer, H.L., Schuster, R., Walston, J., Ray, J.C., Robinson, J.G., Callow, M., et al. (2020). Anthropogenic modification of forests means only 40% of remaining forests have high ecosystem integrity. *Nat. Commun.* 11, 5978. <https://doi.org/10.1038/s41467-020-19493-3>.
27. FAO (2023). Food balance sheets. <https://www.fao.org/faostat/en/#data/FBS> [Accessed: (2024-06-13)].
28. Kastner, T., Matej, S., Forrest, M., Gingrich, S., Haberl, H., Hickler, T., Krausmann, F., Lasslop, G., Niedertscheider, M., Plutzar, C., et al. (2022). Land use intensification increasingly drives the spatiotemporal patterns of the global human appropriation of net primary production in the last century. *Glob. Chang. Biol.* 28, 307–322. <https://doi.org/10.1111/gcb.15932>.
29. Siebert, S., Kummu, M., Porkka, M., Döll, P., Ramankutty, N., and Scanlon, B.R. (2015). A global data set of the extent of irrigated land from 1900 to 2005. *Hydrol. Earth Syst. Sci.* 19, 1521–1545. <https://doi.org/10.5194/hess-19-1521-2015>.
30. Salmon, J.M., Friedl, M.A., Frolking, S., Wisser, D., and Douglas, E.M. (2015). Global rain-fed, irrigated, and paddy croplands: A new high resolution map derived from remote sensing, crop inventories and climate data. *Int. J. Appl. Earth Obs. Geoinf.* 38, 321–334. <https://doi.org/10.1016/j.jag.2015.01.014>.
31. Meier, J., Zabel, F., and Mauser, W. (2018). A global approach to estimate irrigated areas – a comparison between different data and statistics. *Hydrol. Earth Syst. Sci.* 22, 1119–1133. <https://doi.org/10.5194/hess-22-1119-2018>.
32. Chen, Y., Feng, X., Fu, B., Shi, W., Yin, L., and Lv, Y. (2019). Recent global cropland water consumption constrained by observations. *Water Resour. Res.* 55, 3708–3738. <https://doi.org/10.1029/2018WR023573>.
33. Droppers, B., Franssen, W.H.P., van Vliet, M.T.H., Nijssen, B., and Ludwig, F. (2020). Simulating human impacts on global water resources using vic-5. *Geosci. Model Dev. (GMD)* 13, 5029–5052. <https://doi.org/10.5194/gmd-13-5029-2020>.
34. McDermid, S., Nocco, M., Lawston-Parker, P., Keune, J., Pokhrel, Y., Jain, M., Jägermeyr, J., Brocca, L., Massari, C., Jones, A.D., et al. (2023). Irrigation in the Earth system. *Nat. Rev. Earth Environ.* 4, 435–453. <https://doi.org/10.1038/s43017-023-00438-5>.
35. Zhang, X., Zou, T., Lassaletta, L., Mueller, N.D., Tubiello, F.N., Lisk, M.D., Lu, C., Conant, R.T., Dorich, C.D., Gerber, J., et al. (2021). Quantification of global and national nitrogen budgets for crop production. *Nat. Food* 2, 529–540. <https://doi.org/10.1038/s43016-021-00318-5>.
36. Bouwman, L., Goldewijk, K.K., Van Der Hoek, K.W., Beusen, A.H.W., Van Vuuren, D.P., Willems, J., Rufino, M.C., and Stehfest, E. (2013). Exploring global changes in nitrogen and phosphorus cycles in agriculture induced by livestock production over the 1900–2050 period. *Proc. Natl. Acad. Sci. USA* 110, 20882–20887. <https://doi.org/10.1073/pnas.1012878108>.
37. FAO, F. (2020). Livestock and Environment Statistics: Manure and GHG Emissions. In *Global, Regional and Country Trends, 1990–2018, 14 (FAOSTAT Analytical Brief Series)*.
38. Zaehle, S., Friend, A.D., Friedlingstein, P., Dentener, F., Peylin, P., and Schulz, M. (2010). Carbon and nitrogen cycle dynamics in the O-CN land surface model: 2. Role of the nitrogen cycle in the historical terrestrial carbon balance. *Glob. Biogeochem. Cycles* 24, 1–14. <https://doi.org/10.1029/2009GB003522>.
39. Beusen, A.H.W., Van Beek, L.P.H., Bouwman, A.F., Mogollón, J.M., and Middelburg, J.J. (2015). Coupling global models for hydrology and nutrient loading to simulate nitrogen and phosphorus retention in surface water &

- description of image-gnm and analysis of performance. *Geosci. Model Dev. (GMD)* 8, 4045–4067. <https://doi.org/10.5194/gmd-8-4045-2015>.
40. Dietrich, J.P., Mishra, A., Weindl, I., Bodirsky, B.L., Wang, X., Baumstark, L., Kreidenweis, U., Klein, D., Steinmetz, N., Chen, D., et al. (2024). *mrland: MadRaT land data package*. <https://doi.org/10.5281/zenodo.3822083.Rpackageversion0.59.0>.
 41. Ostberg, S., Müller, C., Heinke, J., and Schaphoff, S. (2023). Landing 1.0: a toolbox to derive input datasets for terrestrial ecosystem modelling at variable resolutions from heterogeneous sources. *Geosci. Model Dev. (GMD)* 16, 3375–3406. <https://doi.org/10.5194/gmd-16-3375-2023>.
 42. FAO (2022). FRA 2020 Remote Sensing Survey186 (FAO). <https://doi.org/10.4060/cb9970en>.
 43. Sandström, V., Kaseva, J., Porkka, M., Kuisma, M., Sakieh, Y., and Kahiluoto, H. (2023). Disparate history of transgressing planetary boundaries for nutrients. *Glob. Environ. Change* 78, 102628. <https://doi.org/10.1016/j.gloenvcha.2022.102628>.
 44. Chang, J., Havlík, P., Leclère, D., de Vries, W., Valin, H., Deppermann, A., Hasegawa, T., and Obersteiner, M. (2021). Reconciling regional nitrogen boundaries with global food security. *Nat. Food* 2, 700–711. <https://doi.org/10.1038/s43016-021-00366-x>.
 45. Harris, I., Jones, P.d., Osborn, T.j., and Lister, D.h. (2014). Updated high-resolution grids of monthly climatic observations – the CRU TS3.10 dataset. *Int. J. Climatol.* 34, 623–642. <https://doi.org/10.1002/joc.3711>.
 46. Friedlingstein, P., O'Sullivan, M., Jones, M.W., Andrew, R.M., Bakker, D.C. E., Hauck, J., Landschützer, P., Le Quéré, C., Luijckx, I.T., Peters, G.P., et al. (2023). Global carbon budget 2023. *Earth Syst. Sci. Data* 15, 5301–5369. <https://doi.org/10.5194/essd-15-5301-2023>.
 47. Morseletto, P. (2017). Analysing the influence of visualisations in global environmental governance. *Environ. Sci. Pol.* 78, 40–48. <https://doi.org/10.1016/j.envsci.2017.08.021>.
 48. Mahecha, M.D., Kraemer, G., and Cramer, F. (2024). Cautionary remarks on the planetary boundary visualisation. *Earth Syst. Dyn.* 15, 1153–1159. <https://doi.org/10.5194/esd-15-1153-2024>.
 49. Rockström, J., Kotzé, L., Milutinović, S., Biermann, F., Brovkin, V., Donges, J., Ebbesson, J., French, D., Gupta, J., Kim, R., et al. (2024). The planetary commons: A new paradigm for safeguarding Earth-regulating systems in the Anthropocene. *Proc. Natl. Acad. Sci.* 121, e2301531121. <https://doi.org/10.1073/pnas.2301531121>.
 50. Rockström, J., Steffen, W., Noone, K., Persson, A., Chapin, F.S.I., Lambin, E., Lenton, T., Scheffer, M., Folke, C., Schellnhuber, H.J., et al. (2009). Planetary Boundaries: Exploring the Safe Operating Space for Humanity. *Ecol. Soc.* 14. <https://doi.org/10.5751/ES-03180-140232>.
 51. Springmann, M., Clark, M., Mason-D'Croz, D., Wiebe, K., Bodirsky, B.L., Lassaletta, L., de Vries, W., Vermeulen, S.J., Herrero, M., Carlson, K.M., et al. (2018). Options for keeping the food system within environmental limits. *Nature* 562, 519–525. <https://doi.org/10.1038/s41586-018-0594-0>.
 52. Vea, E.B., Richardson, K., Bjørn, A., and Hauschild, M. (2025). Approaches for aggregating data from the regional to the global level: importance for conclusions on Earth system state. *Environ. Res. Lett.* 20, 033001. <https://doi.org/10.1088/1748-9326/adaae8>.
 53. Bai, X., Hasan, S., Andersen, L.S., Bjørn, A., Kilkiş, Ş., Ospina, D., Liu, J., Cornell, S.E., Sabag Muñoz, O., de Bremond, A., et al. (2024). Translating Earth system boundaries for cities and businesses. *Nat. Sustain.* 7, 108–119. <https://doi.org/10.1038/s41893-023-01255-w>.
 54. Leng, G., and Hall, J.W. (2021). Where is the planetary boundary for freshwater being exceeded because of livestock farming? *Sci. Total Environ.* 760, 144035. <https://doi.org/10.1016/j.scitotenv.2020.144035>.
 55. Lade, S.J., Steffen, W., de Vries, W., Carpenter, S.R., Donges, J.F., Gerten, D., Hoff, H., Newbold, T., Richardson, K., and Rockström, J. (2019). Human impacts on planetary boundaries amplified by Earth system interactions. *Nat. Sustain.* 3, 119–128. <https://doi.org/10.1038/s41893-019-0454-4>.
 56. Chrysafi, A., Virkki, V., Jalava, M., Sandström, V., Piipponen, J., Porkka, M., Lade, S.J., La Mere, K., Wang-Erlandsson, L., Scherer, L., et al. (2022). Quantifying Earth system interactions for sustainable food production via expert elicitation. *Nat. Sustain.* 5, 830–842. <https://doi.org/10.1038/s41893-022-00940-6>.
 57. Drüke, M., von Bloh, W., Petri, S., Sakschewski, B., Schaphoff, S., Forkel, M., Huiskamp, W., Feulner, G., and Thonicke, K. (2021). Cm2mc-lpjml v1.0: biophysical coupling of a process-based dynamic vegetation model with managed land to a general circulation model. *Geosci. Model Dev. (GMD)* 14, 4117–4141. <https://doi.org/10.5194/gmd-14-4117-2021>.
 58. Tomalka, J., Hunecke, C., Murken, L., Heckmann, T., Cronauer, C.C., Becker, R., Collignon, Q., Collins-Sowah, P.A., Crawford, M., Gloy, N., et al. (2024). Stepping back from the precipice: Transforming land management to stay within planetary boundaries. Technical report. <https://doi.org/10.48485/pik.2024.018>.
 59. Dixon-Declève, S., Gaffney, O., Ghosh, J., Randers, J., Rockstrom, J., and Stoknes, P.E. (2022). *Earth for All: A Survival Guide for Humanity* (New society Publishers).
 60. Frieler, K., Volkholz, J., Lange, S., Schewe, J., Mengel, M., del Rocío Rivas López, M., Otto, C., Reyer, C.P.O., Karger, D.N., Malle, J.T., et al. (2024). Scenario setup and forcing data for impact model evaluation and impact attribution within the third round of the inter-sectoral impact model inter-comparison project (ISIMIP3a). *Geosci. Model Dev. (GMD)* 17, 1–51. <https://doi.org/10.5194/gmd-17-1-2024>.
 61. Wirth, S.B., Braun, J., Heinke, J., Ostberg, S., Rolinski, S., Schaphoff, S., Stenzel, F., von Bloh, W., Taube, F., and Müller, C. (2024). Biological nitrogen fixation of natural and agricultural vegetation simulated with lpjmL 5.7.9. *Geosci. Model Dev. (GMD)* 17, 7889–7914. <https://doi.org/10.5194/gmd-17-7889-2024>.
 62. Kim, H. (2017). Global soil wetness project phase 3 (gswp3) - atmospheric boundary conditions. <https://doi.org/10.20783/DIAS.501>.
 63. Lange, S. (2019). WFDE5 over land merged with ERA5 over the ocean (W5E5). v. 1.0. GFZ Data Services. <https://doi.org/10.5880/pik.2019.023>.
 64. Flörke, M., Kynast, E., Bärlund, I., Eisner, S., Wimmer, F., and Alcamo, J. (2013). Domestic and industrial water uses of the past 60 years as a mirror of socio-economic development: A global simulation study. *Glob. Environ. Change* 23, 144–156. <https://doi.org/10.1016/j.gloenvcha.2012.10.018>.
 65. Porwollik, V., Rolinski, S., Heinke, J., von Bloh, W., Schaphoff, S., and Müller, C. (2022). The role of cover crops for cropland soil carbon, nitrogen leaching, and agricultural yields – a global simulation study with LPJmL (v. 5.0-tillage-cc). *Biogeosciences* 19, 957–977. <https://doi.org/10.5194/bg-19-957-2022>.
 66. Herrero, M., Havlík, P., Valin, H., Notenbaert, A., Rufino, M.C., Thornton, P. K., Blümmel, M., Weiss, F., Grace, D., and Obersteiner, M. (2013). Biomass use, production, feed efficiencies, and greenhouse gas emissions from global livestock systems. *Proc. Natl. Acad. Sci. USA* 110, 20888–20893. <https://doi.org/10.1073/pnas.1308149110>.
 67. Heinke, J., Lannerstad, M., Gerten, D., Havlík, P., Herrero, M., Notenbaert, A.M.O., Hoff, H., and Müller, C. (2020). Water Use in Global Livestock Production—Opportunities and Constraints for Increasing Water Productivity. *Water Resour. Res.* 56, e2019WR026995. <https://doi.org/10.1029/2019WR026995>.
 68. Haberl, H., Erb, K.H., Krausmann, F., Gaube, V., Bondeau, A., Plutzar, C., Gingrich, S., Lucht, W., and Fischer-Kowalski, M. (2007). Quantifying and mapping the human appropriation of net primary production in earth's terrestrial ecosystems. *Proc. Natl. Acad. Sci. USA* 104, 12942–12947. <https://doi.org/10.1073/pnas.0704243104>.
 69. Virkki, V., Alanärä, E., Porkka, M., Ahopelto, L., Gleeson, T., Mohan, C., Wang-Erlandsson, L., Flörke, M., Gerten, D., Gosling, S.N., et al. (2022). Globally widespread and increasing violations of environmental flow envelopes. *Hydrolog. Earth Syst. Sci.* 26, 3315–3336. <https://doi.org/10.5194/hess-26-3315-2022>.
 70. Pastor, A.V., Ludwig, F., Biemans, H., Hoff, H., and Kabat, P. (2014). Accounting for environmental flow requirements in global water assessments. *Hydrolog. Earth Syst. Sci.* 18, 5041–5059. <https://doi.org/10.5194/hess-18-5041-2014>.

71. de Vries, W., Schulte-Uebbing, L., Kros, H., Voogd, J.C., and Louwagie, G. (2021). Spatially explicit boundaries for agricultural nitrogen inputs in the European Union to meet air and water quality targets. *Sci. Total Environ.* 786, 147283. <https://doi.org/10.1016/j.scitotenv.2021.147283>.
72. de Vries, W., Kros, J., Kroeze, C., and Seitzinger, S.P. (2013). Assessing planetary and regional nitrogen boundaries related to food security and adverse environmental impacts. *Curr. Opin. Environ. Sustain.* 5, 392–402. <https://doi.org/10.1016/j.cosust.2013.07.004>.
73. Wickham, H., Hester, J., Chang, W., and Bryan, J. (2022). devtools: Tools to Make Developing R Packages Easier. <https://CRAN.R-project.org/package=devtools.Rpackageversion2.4.5>.
74. Braun, J., Breier, J., Stenzel, F., and Vanelli, C. (2024). boundaries: Planetary Boundary Status based on LPJmL Simulations (Version 1.0.1) [Computer software]. <https://doi.org/10.5281/zenodo.11550559>. <https://github.com/pik-tess/boundaries>.

One Earth, Volume 8

Supplemental information

**A software package for assessing
terrestrial planetary boundaries**

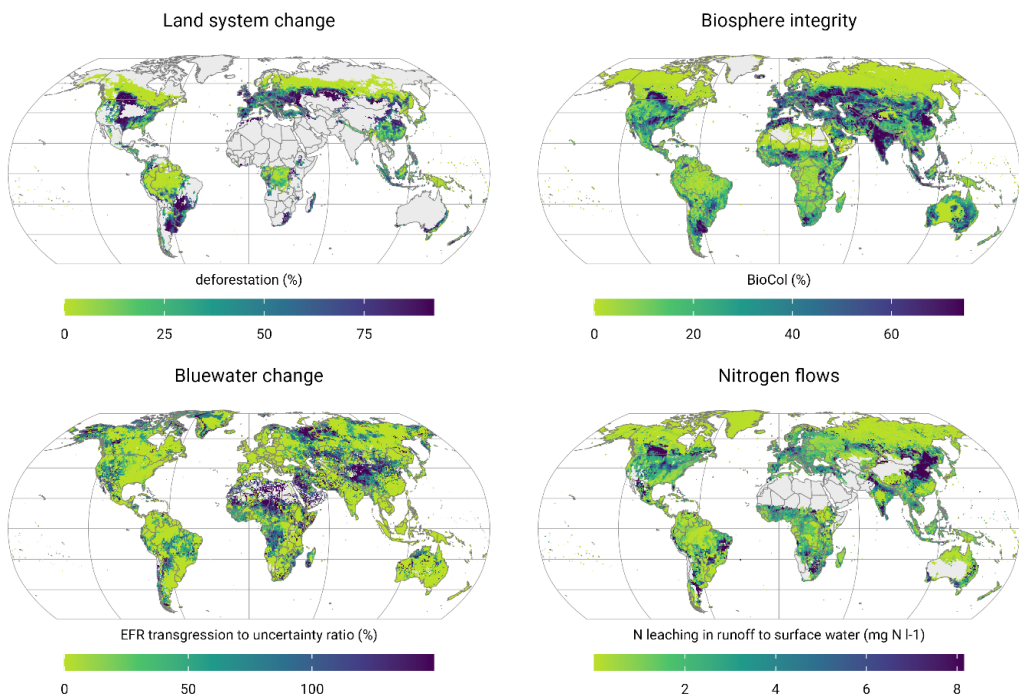
Dieter Gerten, Johanna Braun, Jannes Breier, Wolfgang Lucht, Arne Tobian, and Fabian Stenzel

Supplemental Information

Dieter Gerten, Johanna Braun, Jannes Breier, Wolfgang Lucht, Arne Tobian, and Fabian Stenzel: A software package for assessing terrestrial planetary boundaries, One Earth, 2025

Supplemental Figures

A



B

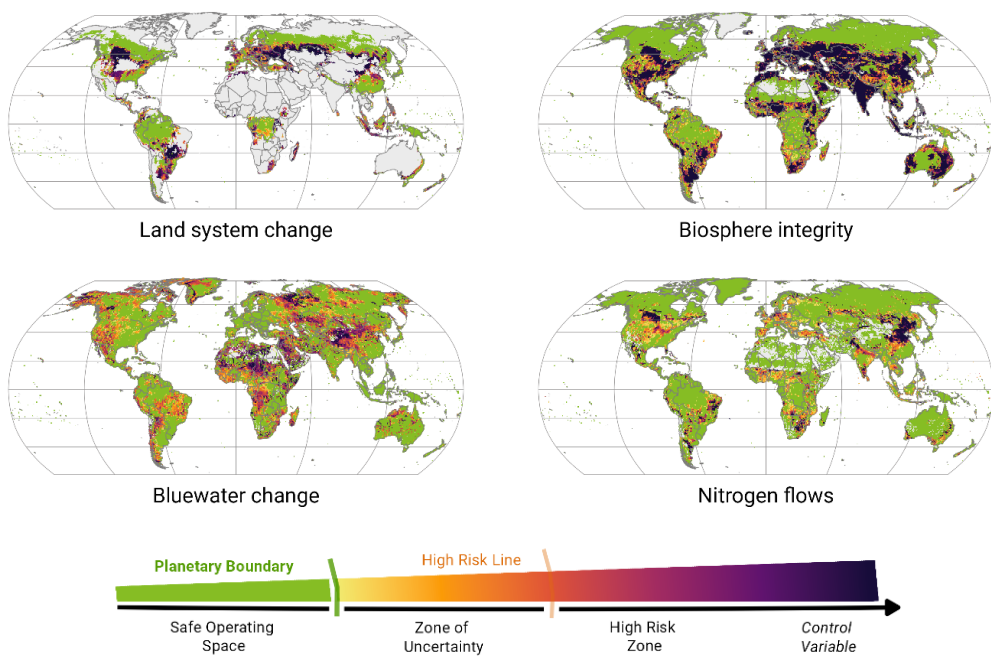
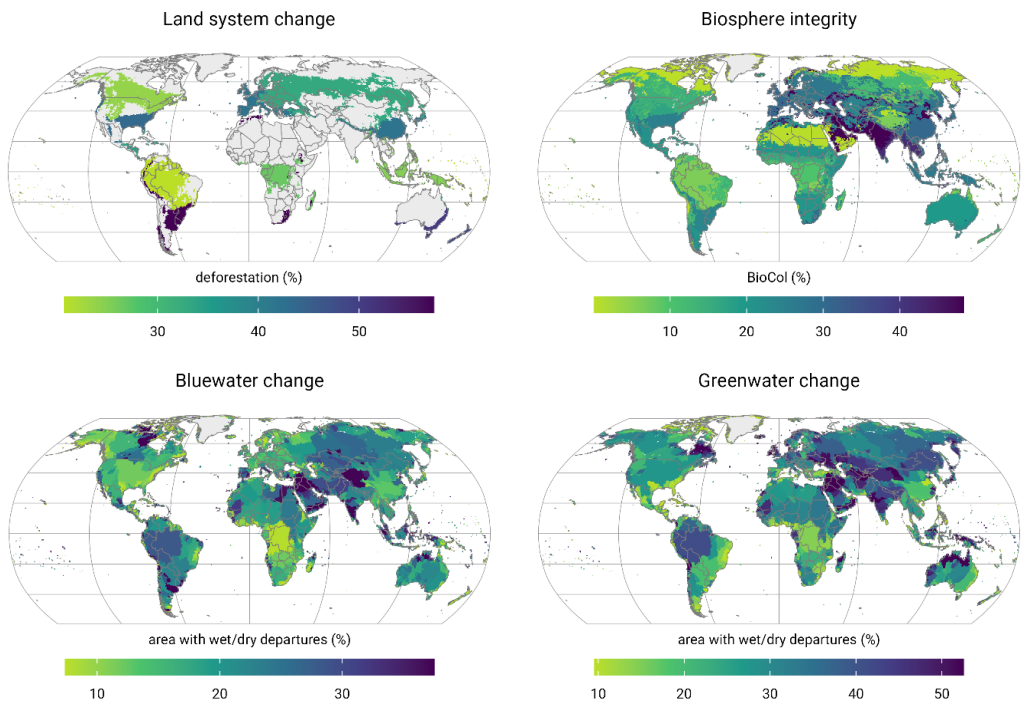


Figure S1: Gridded patterns of statuses of the four planetary boundaries analyzed. (A) PB control variables; (B) PB statuses based on conversion to a normalized risk level, cf. Figure 3 in the main text.

A



B

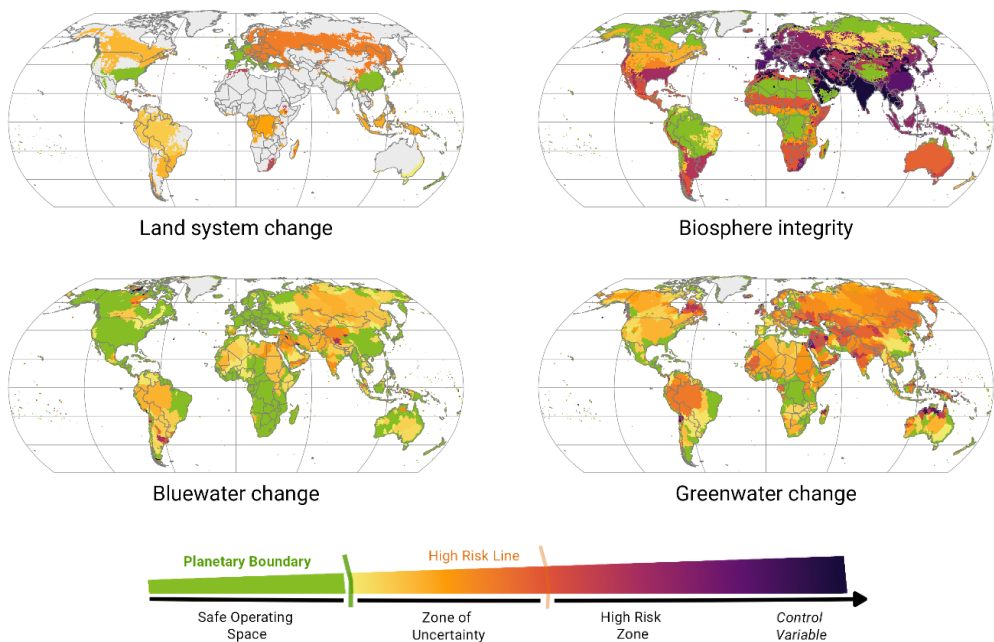


Figure S2: Regional (biome- and river basin-scale) PB statuses. (A) PB control variables; (B) PBs based on conversion to a normalized risk level, cf. Figure 3 and using outlines from Figure S3. Results should be cautiously interpreted for green and blue water change because of small basins at the continent shelves, occurring due to the specific river drainage directions used.

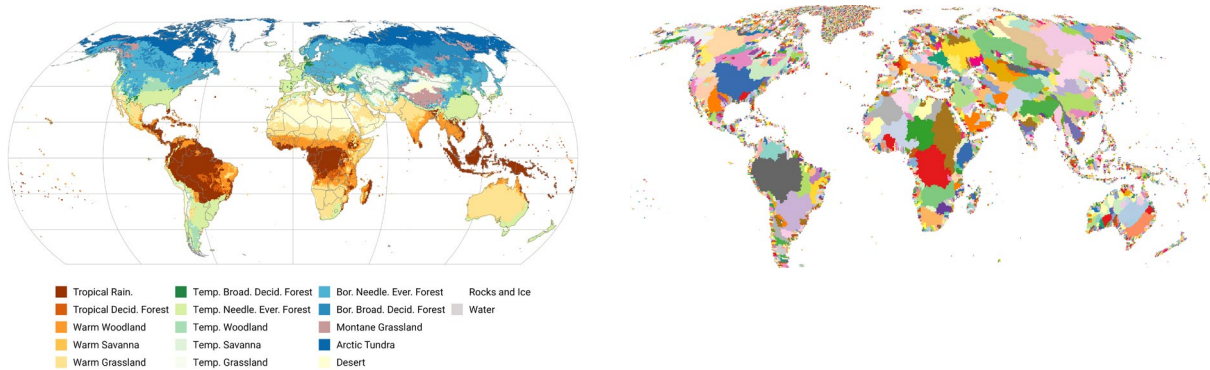


Figure S3: Delineations of terrestrial biomes (left) and river basins (right; colors only demarcate the different basins) used for regional aggregation (in Figures 3 and Figure S2, respectively).

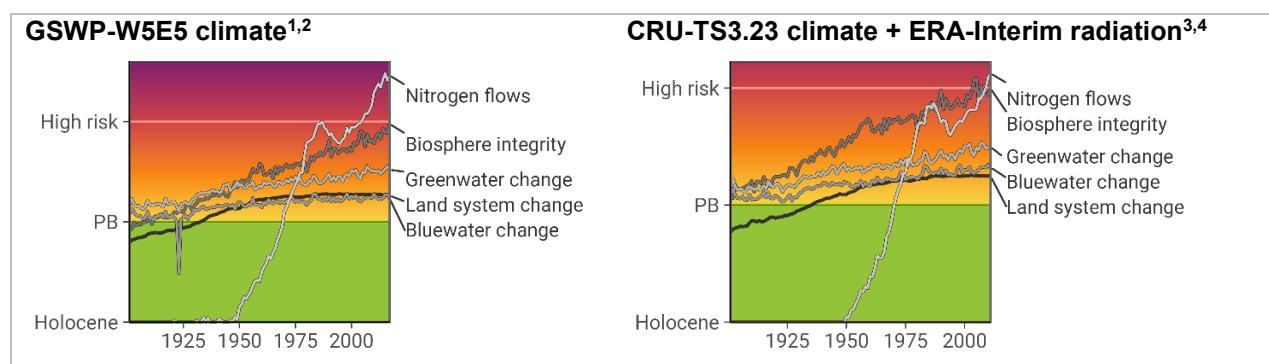


Figure S4: PB status development over time, simulated under different climate input datasets (GSWP3 vs. CRU; left-panel plot same as in Figure 2, used here for comparison).

Supplemental Tables

LPJmL identifier	Description	PBs (spatial scale)	ISIMIP variable
Grid	Center coordinates (latitude, longitude) for the used grid	All	*
terr_area	Total land area of a grid cell (excluding water bodies)	All	*
temp	Near-surface air temperature	Biome classification, blue / green water	tas
prec	Precipitation	Nitrogen (N) (grid)	pr
elevation	Elevation	Biome classification	*

Natural vegetation related

fpc	Foliar projected cover of natural plant functional types	Biome classification, blue/green water, biosphere integrity, land-system change	pft-<pft>
vegc	Carbon mass in vegetation	Biome classification	cveg-total
pft_lai	Leaf area index of natural plant functional types	Biome classification	lai-<pft>
npp	Carbon Mass Flux out of Atmosphere due to Net Primary Production on Land	Biosphere integrity	npp-total

pft_npp	Net primary production of natural plant functional types	Biosphere integrity	npp-<pft>
Water related			
runoff	Total (surface + subsurface) runoff	Nitrogen (grid)	qtot
pet	Potential evapotranspiration	Nitrogen (grid)	potevap
discharge	River discharge (accumulated runoff along the river network)	Blue water	dis
bcons_irr	Actual Irrigation Water (blue water) Consumption	Blue water (global, based on irrigation consumption)	airruse
wateruse_hil	Blue water consumption from households, industry and live-stock	Blue water (global, based on irrigation consumption)	amanuse + aelecuse + adomuse + aliveuse
rootmoist	Plant available soil moisture / soil moisture content at root zone	Green water	rootmoist
drainage	Drainage map / flow direction	Blue / green water (basin level)	*
Nitrogen related			
leaching	Total N loss in runoff and leaching	Nitrogen (grid)	fnleach
napplied_mg	Total N in manure and fertilizer applied on agricultural land (managed grassland and cropland)	Nitrogen (global)	n.a.
bnf_mg	Intentional biological N fixation on agricultural land (managed grassland and cropland)	Nitrogen (global)	n.a.
flux_estabn_mg	N flux from crop/grass establishment on agricultural land (e.g. from seeds)	Nitrogen (global)	n.a.
harvest	N removed from agricultural land (managed grassland and cropland) by harvest	Nitrogen (global)	n.a.
ndepo_mg	N deposition on agricultural land (managed grassland and cropland)	Nitrogen (global)	n.a.

* Essential but model-independent input provided to *boundaries* not provided by ISIMIP. In this paper we take these data from the LPJmL model setup. Alternatively, they can be compiled from open-source data (e.g. EarthExplorer, <https://earthexplorer.usgs.gov>) and provided in netCDF format; for maximum consistency, they should match the spatial resolution of the model variables used.

n.a.: No corresponding ISIMIP variable available.

Table S1: Mapping of LPJmL output variables and related PBs against corresponding variables in the ISIMIP framework (<https://protocol.isimip.org>), related to Box 1 in the main text. Variables required for the biome classification are used to aggregate the grid cell level status to regional level for the PBs for land-system change and biosphere integrity.

Supplemental references

- ¹ Kim, H. (2017). Global Soil Wetness Project Phase 3 (GSWP3) – Atmospheric Boundary Conditions, <https://doi.org/10.20783/DIAS.501>
- ² Lange, S. (2019). WFDE5 over land merged with ERA5 over the ocean (W5E5). V. 1.0, <https://doi.org/10.5880/pik.2019.023>
- ³ Harris, I.; Jones, P.; Osborn, T. & Lister, D. (2014). Updated high-resolution grids of monthly climatic observations – the CRU TS3.10 Dataset. International Journal of Climatology, 34, 623-642, <https://doi.org/10.1002/joc.3711>
- ⁴ Berrisford, P.; Dee, D.; Poli, P.; Brugge, R.; Fielding, M.; Fuentes, M.; Källberg, P.; Kobayashi, S.; Uppala, S. & Simmons, A. (2011). The ERA-Interim archive Version 2.0, ERA Report Series, <https://www.ecmwf.int/en/elibrary/73682-era-interim-archive-version-20>